Nanocomposite Materials Design Optimization at Multiple Length-Scales

Part II: Composite Processing and Properties

Rajendra Bordia, Co-PI

Shelly Arreguin, Kevin Strong and Kaishi Wang

University of Washington Seattle, Washington

Supported By

The Air Force Office of Scientific Research- AFOSR FA9550-09-0633

Program Manager: Dr. Joan Fuller and Dr. Ali Sayir

Nanocomposite Materials Design Optimization with Experimental Validation for Engineered Microstructure at Multiple Length-Scales (AFOSR FA9550-09-1-0633)

Co-PI: Rajendra Bordia
University of Washington, Seattle, WA

Experimental Validation

STATUS QUO

Experimentally intensive materials development

- Design of microstructure by trial and error
- Broad guidelines but no protocol for optimization
- Limited parameter space explored

NEW INSIGHTS

Microstructure Optimization

- Multiscale simulations approaches for properties of composite ceramics
- Varying fidelity optimization approaches for design of optimal microstructures
- Development of processing approaches to make a nanoscale SiC reinforced Si_3N_4 matrix composites.

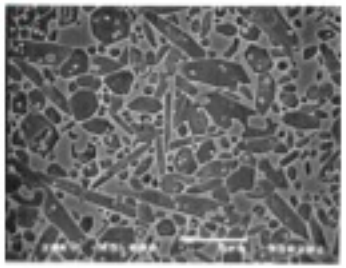

Figure 1: SiC-Si_3N_4 inter/intra composites using powder processing and gas pressure sintering

- Nano-scale SiC improves the creep resistance of Si_3N_4

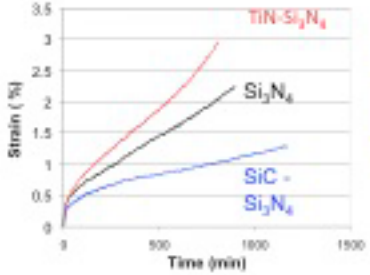

Figure 2: Compressive creep at 1325°C under 200 MPa stress

MAIN ACHIEVEMENTS:

- Exploration of effect of polymer composition on nano-composite phase composition
- Development of a two-step pyrolysis process to control nano-composite phase composition

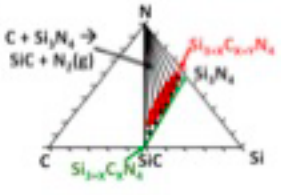

Figure 3:. Effect of polymer composition on ceramic phases

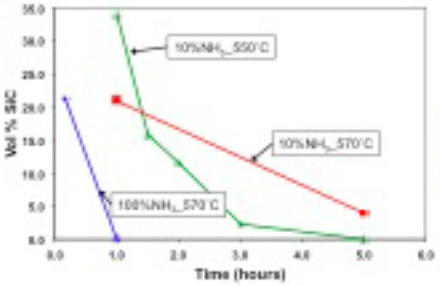

Figure 4: Two-step pyrolysis to control composition of ceramic phases

HOW IT WORKS:

- For polymer compositions in the N-SiC-Si_3N_4 triangle, carbothermic reduction pushes equilibrium composition to be on the SiC-Si_3N_4 line (Figure 3).
- Low temperature heat treatment in different environment leads to control of composition (Figure 4) due to substitution reaction (Figure 5).

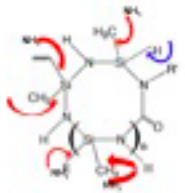

Figure 5: At intermediate temperature (around 500 °C, NH_3 attacks both Si-H and Si-C bonds leading to reduction in C and increase in N in the heat treated ceramic

QUANTITATIVE IMPACT — END-OF-PHASE GOAL

Current Impact

- Processing protocols to make SiC-Si_3N_4 composites (with SiC content between 0 – 25 vol. %) have been developed
- The room temperature mechanical properties (strength and fracture toughness) has been measured for selected composite microstructures and the effect of reinforcement quantified
- Creep resistance of SiC reinforced composites is 100 times better than that of Si_3N_4

Planned Impact

- A robust design optimization capable of predicting optimal SiC-Si_3N_4 microstructures under uncertain processing and operating environments.
- Experimental validation of models and design procedure.

Research Goals

Development and experimental validation of a numerical tool to optimally design multiscale nanocomposites based on direct correlation with processing and experiments.

Publications

- K. Wang, M. Günter, G. Motz and R.K. Bordia, **J Euro Cer Soc, 31** 3011-3020 (2011).
- M. Günthner, K. Wang, R. K. Bordia, and G. Motz, **J. Euro Cer Soc, 32**, 1883-1892 (2012).
- R. K. Bordia and H. Camacho-Montes, Chapter in *Ceramics and Composites Processing Methods*, **Eds. Narottam Bansal and Aldo R. Boccaccini**, 3-42 John Wiley & Sons (2012).
- K.Wang, X.Zheng, F.S. Ohuchi and R.K. Bordia, **Rapid Communication J. Am. Cer. Soc. 95** [12] 3722-3725 (2012).
- 4 papers under preparation – more planned
- 3 papers from the Tomar group used materials supplied by our group

Classes of Nanocomposite

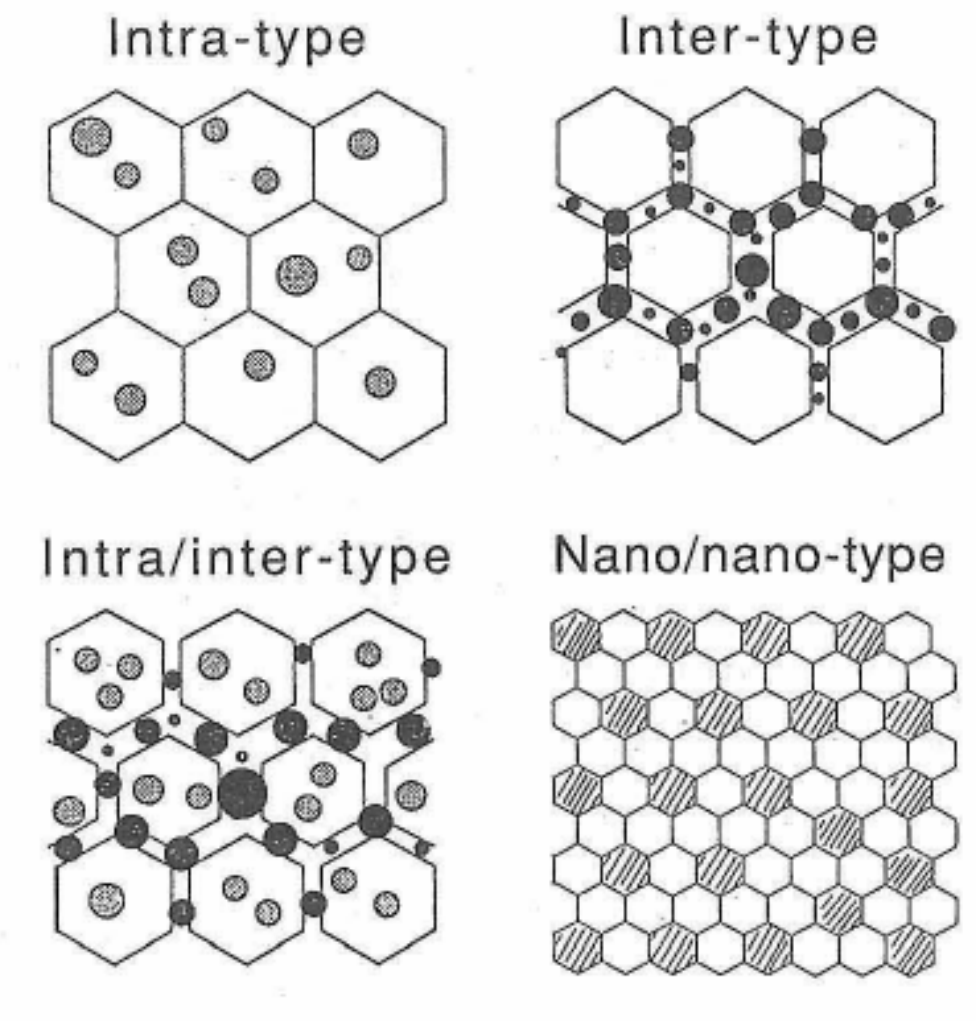

Niihara, *J. Cerm. Soc. Jap.*, 99 [10] (1991) p. 974.

Simulation Guided Materials Development

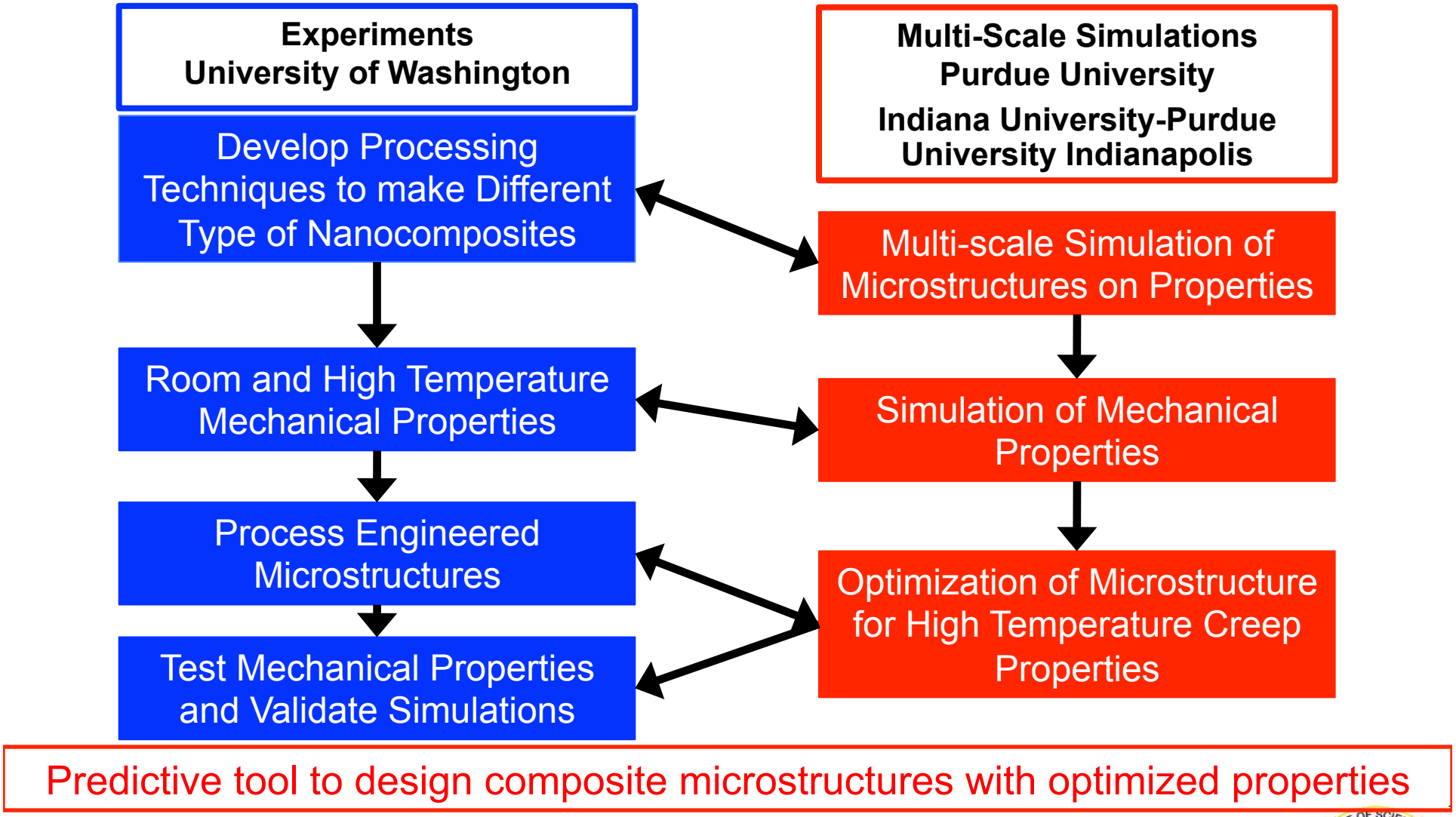

Predictive tool to design composite microstructures with optimized properties

Outline of the Research at UW

- Nano-composites using Powder Processing (Intra/Inter)
  - Processing
  - Microstructure Evolution
  - Room and High Temperature Properties

- Nano-composites using Molecular Precursor
  - Processing of SiC-Si_3N_4 Composites with Controlled Volume Fraction of SiC over a Broad Range
  - Effect of Temperature and Atmosphere on the Phase Evolution
  - Microstructural Development (ongoing)

- Composite Coatings (Summary)
  - Processing of Coatings
  - Mechanical, Environmental and Surface Properties of Coatings

Powder Processing of Nano-composites

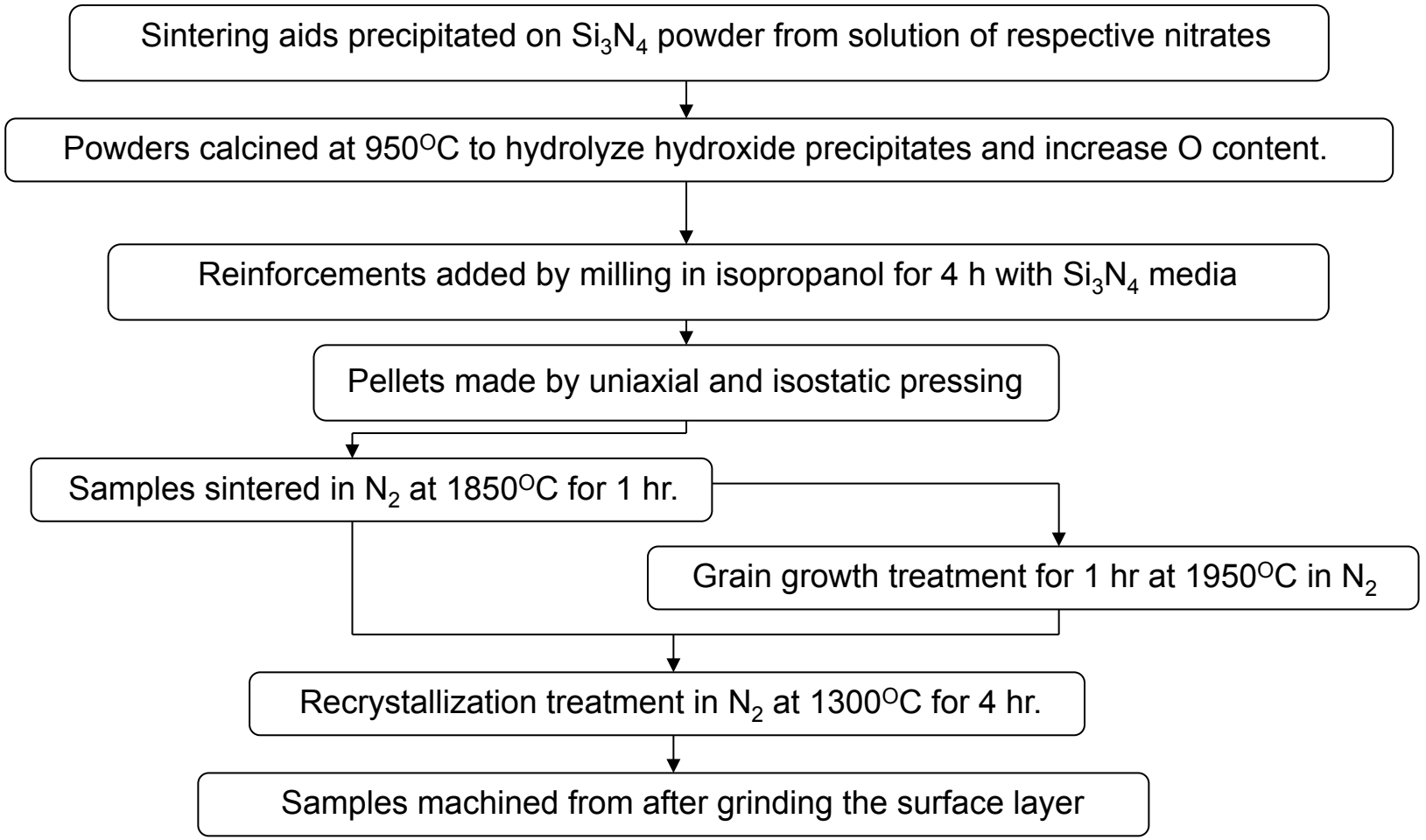

Matrix: Si_3N_4 + 10 mole % 5:3 Al_2O_3 : Y_2O_3

Reinforcement: 10 vol.% SiC, or TiN nanoparticles

Microstructure of Intra/Inter Nano-composites

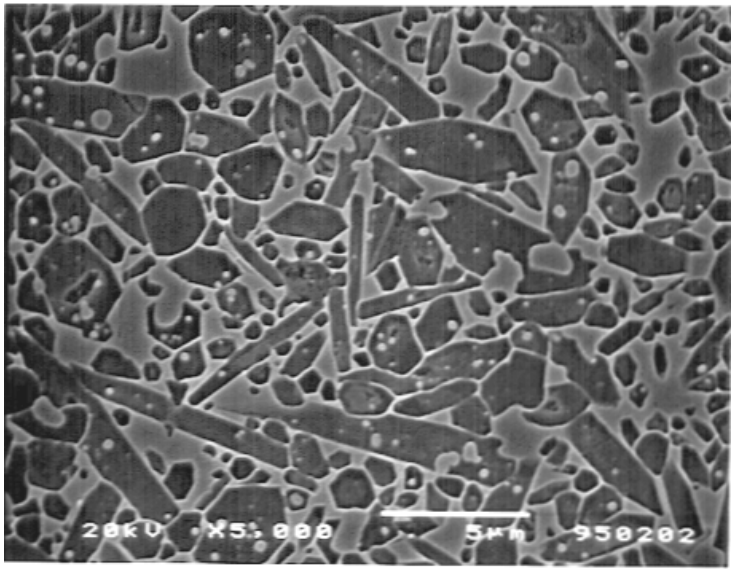

SiC-Si_3N_4

- Fully dense microstructures obtained for Si_3N_4 and composites (β-Si_3N_4).
- Reinforcements located both within Si_3N_4 grains and at grain boundaries.
- SiC particles seen predominantly within Si_3N_4 grains.
- TiN particles seen predominantly between Si_3N_4 grains.

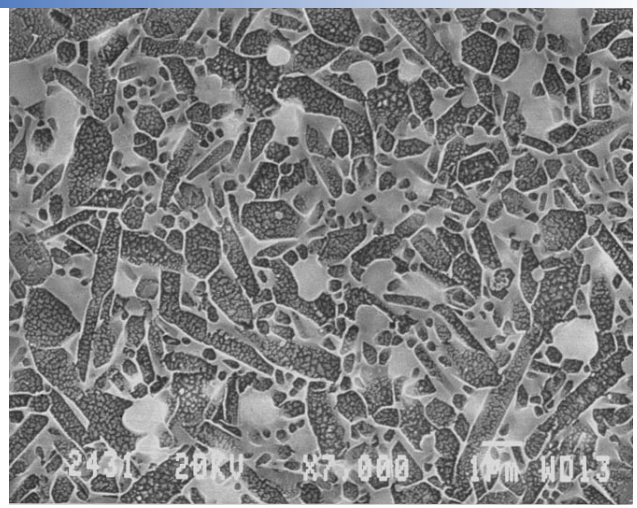

TiN-Si_3N_4 (Secondary electron image)

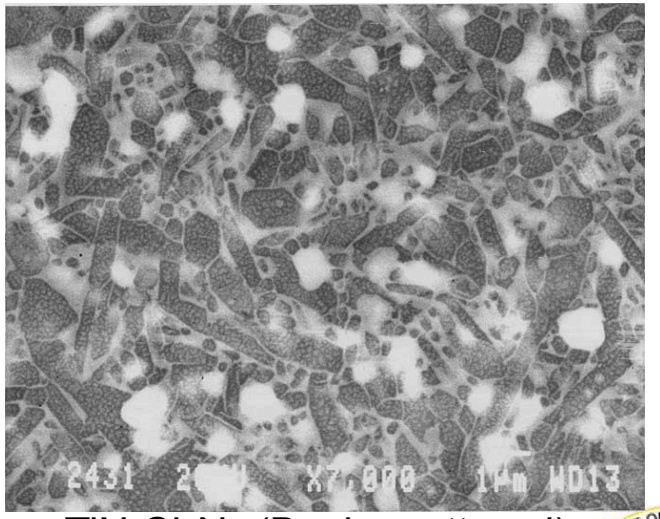

TiN-Si_3N_4 (Back-scattered)

Effect of Heat Treatment on Microstructure

As Sintered

- No significant differences between grain size and aspect ratio of Si_3N_4 and it's composites.
- Average minor size (0.5 μm) and average aspect ratio 2.8
- Intra/Inter nano-composites

After Grain Growth Heat Treatment (1 hr. at 1950 ^{0}C)

- No significant differences between grain size and aspect ratio of Si_3N_4 and it's composites.
- Average minor size (0.8 μm) and average aspect ratio 2.2
- Intra/Inter nano-composites

Approximately 60 % increase in minor grain size and 20% decrease in aspect ratio

Room Temperature Mechanical Properties

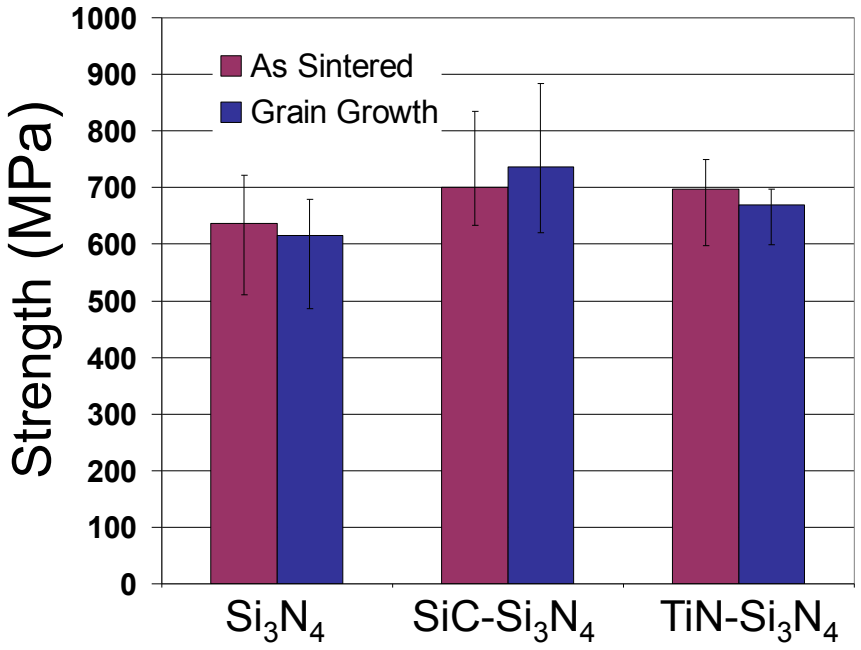

4-pt Flexure Average of 10 measurements

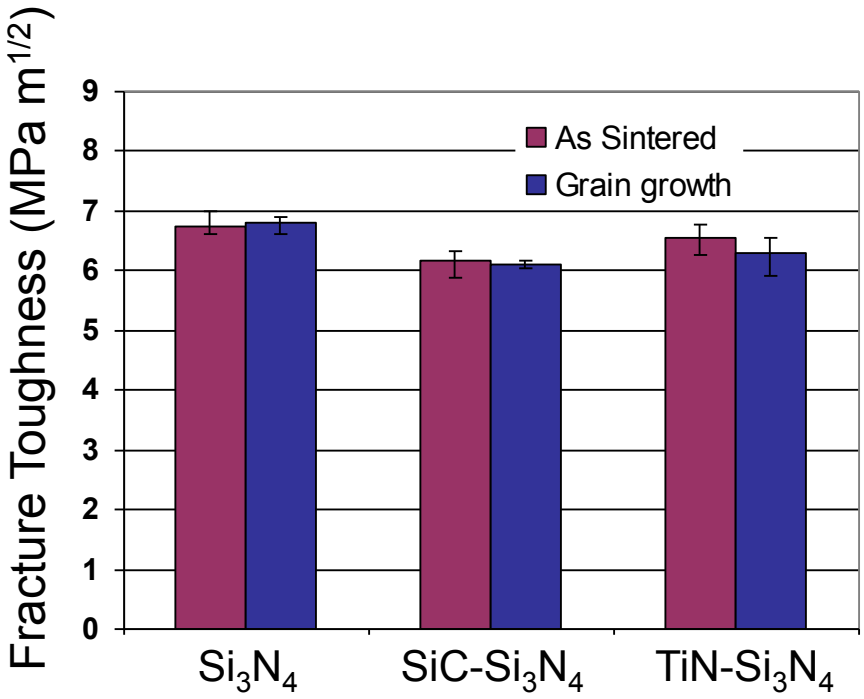

SEVNB Average of 3 measurements

- ~10% improvement in strength on addition of reinforcements.
- Fracture Toughness reduces on addition of reinforcements (~ 5 to10%).
- No significant change in properties after grain growth treatment.

Compressive Creep - Procedure

- Creep tests carried out on 3.5 x 3.5 x 8 mm samples loaded under 200 MPa compressive stress.
- Tests conducted in air at temperatures of 1300^{O}-1375^{O}C.
- Tests conducted on a Universal Testing Machine with an attached high temperature furnace.
- Strain monitored by a One-Arm Contact Extensometer measuring displacement of load train outside furnace.

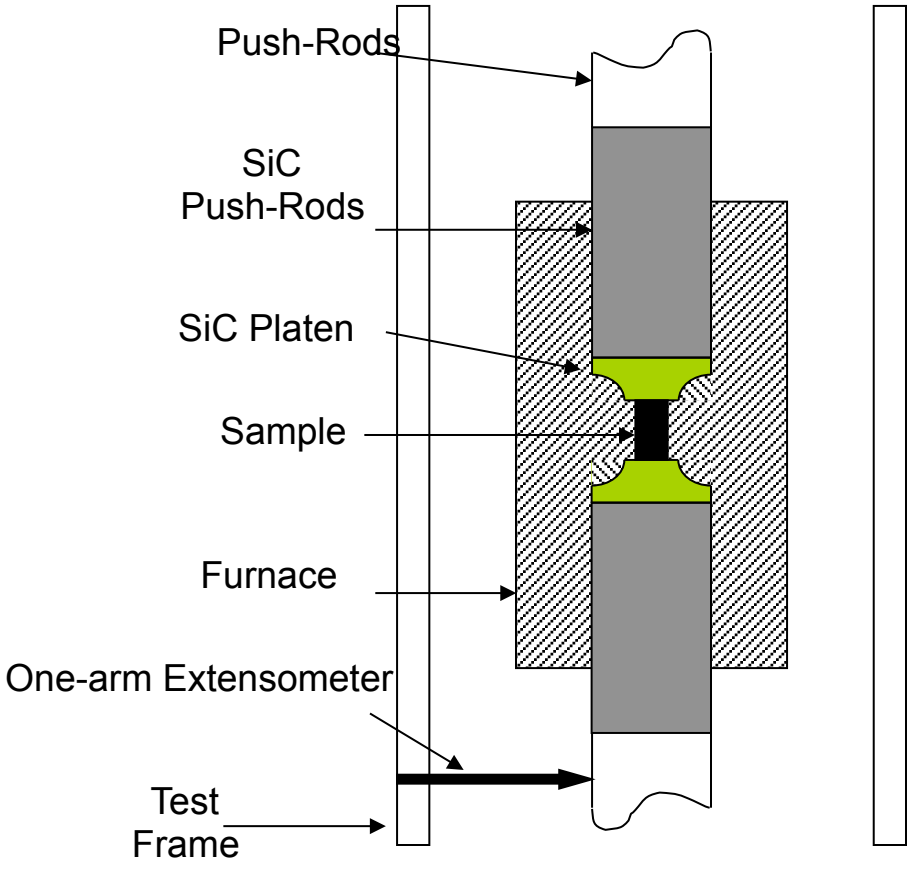

Compressive Creep Results

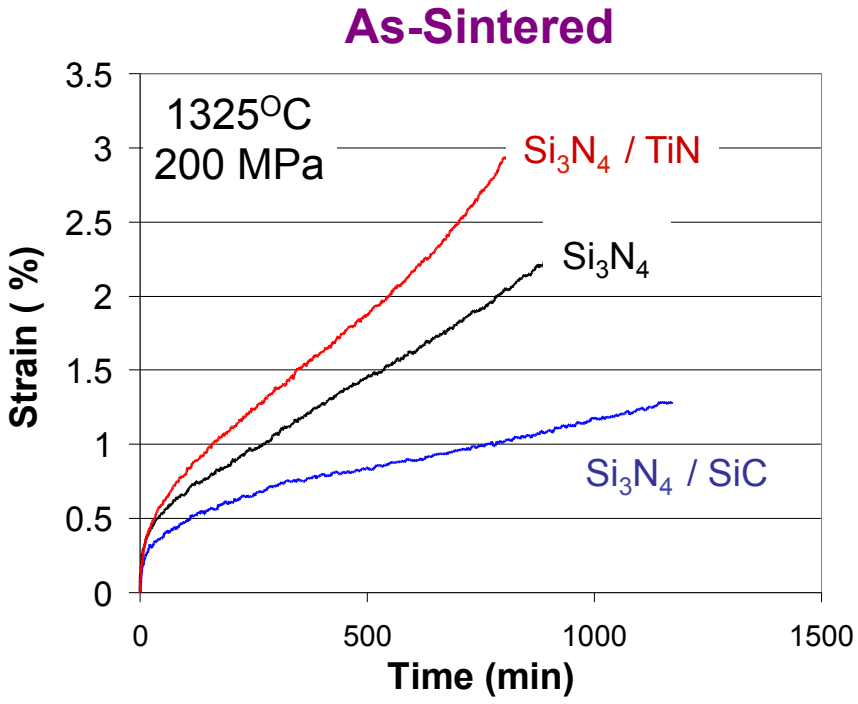

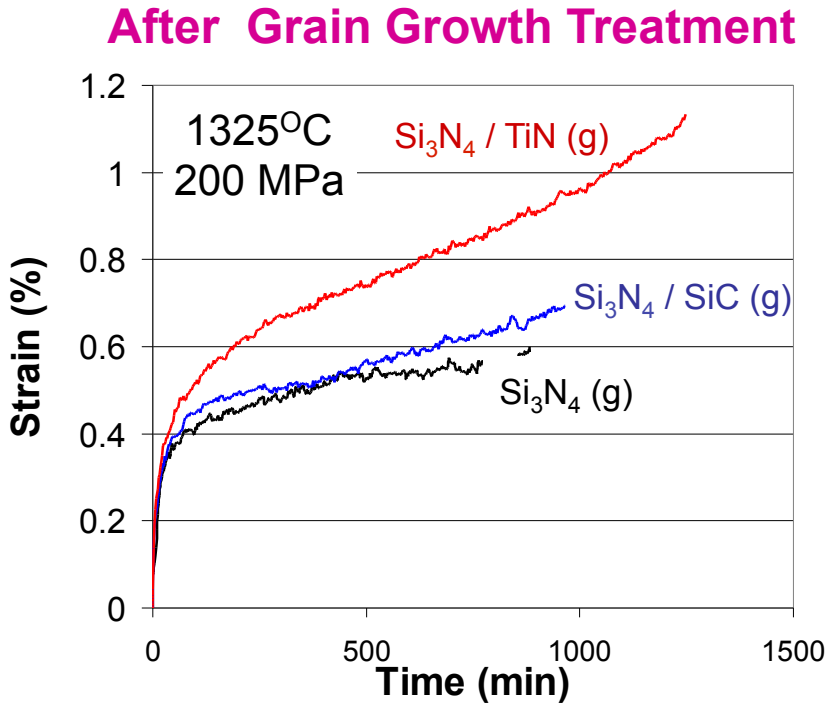

- Addition of SiC results in improved creep resistance in as sintered Si_3N_4; addition of TiN results in poorer creep resistance.
- Steady state creep rates are reduced by about two orders of magnitude after grain growth treatment for all three materials.
- No improvement in creep resistance observed on SiC addition in samples subjected to grain growth treatment; addition of TiN results in poorer creep resistance.

Temperature Dependence of Creep

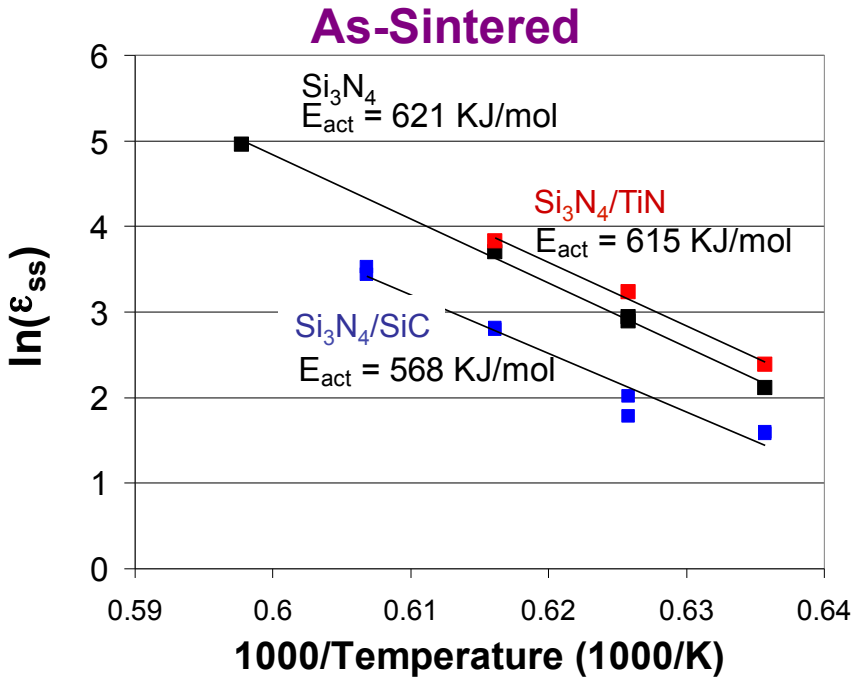

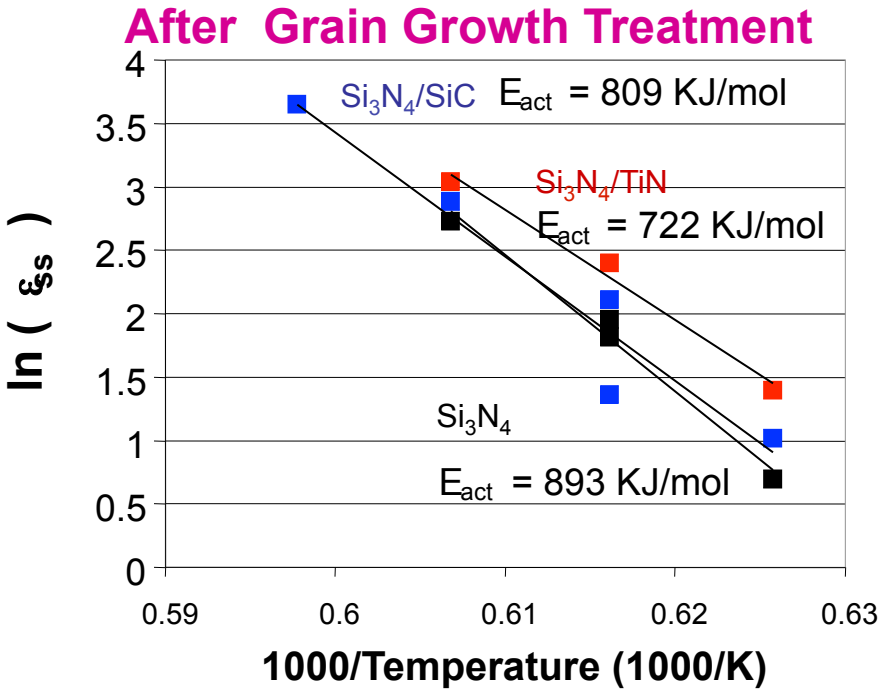

- Activation energies of as-sintered $Si_3N_4$and it's composites are similar (within 5% of 600 KJ/mol).
- For the same material, activation energy is higher after grain growth treatment.
- Observed greater differences in activation energies of Si_3N_4 and it's composites (within $\pm$10% of 800 KJ/mol) than in as-sintered samples.

Summary of Creep of Nano-composites

Mechanism:

- Creep in Si_3N_4 and TiN-Si_3N_4 is diffusion controlled (grain size exponent of 3.2).
- Creep in SiC-Si_3N_4 is controlled by interface reaction (grain size exponent of 1.05).

Possible explanation (Si_3N_4 – TiN nanocomposites):

- Mechanism of creep in Si_3N_4 and TiN-Si_3N_4 is the same
- TiN either reduces grain boundary viscosity or increases solubility of Si_3N_4 in the grain boundary phase – both leading to accelerated creep

Possible explanation (Si_3N_4 – SiC nanocomposites):

- SiC addition changes the rate controlling step (from diffusion controlled to interface controlled)
- Significant improvement in creep resistance for the an-sintered material
- Possible mechanism could be due to change in grain boundary sliding resistance due to pinning effect of SiC.

Nano-composites using Molecular Precursors

Motivation

- Possibly better control of SiC volume fraction
- Possibly better control of microstructure – including ability to make nano-nano composites.

Precursor

KiON® Specialty Polymers
A Clariant Business

Ceraset PURS 20
Polyureasilazane

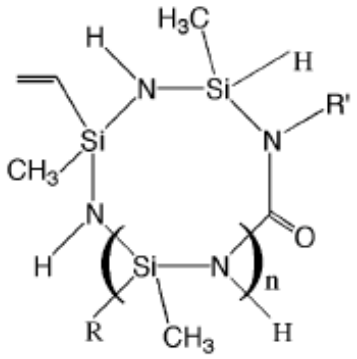

Processing Method (to Control SiC content)

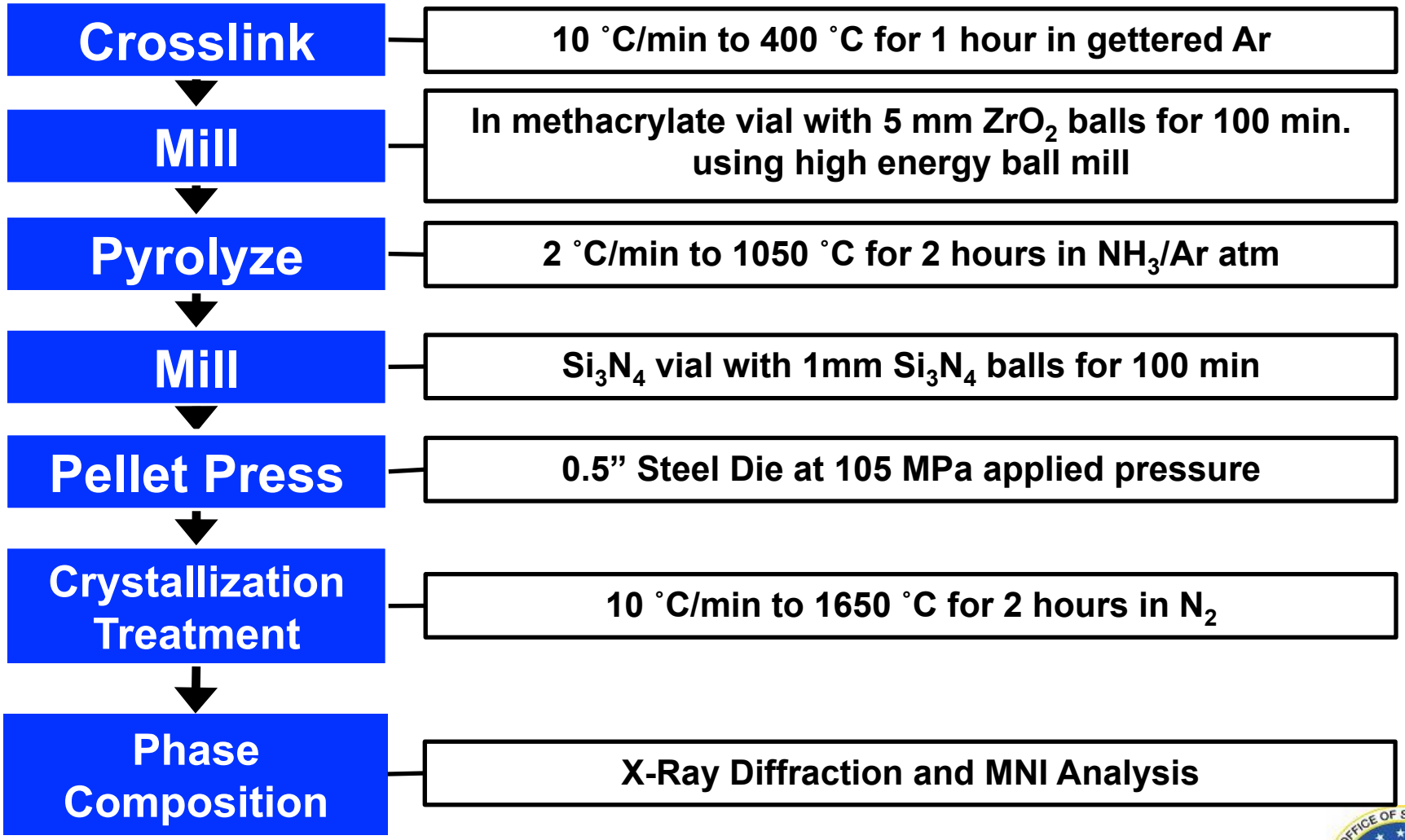

Quantitative Phase Analysis

$$I_{ij} = \frac{K\left(mL_p|F|^2\right)_{ij}\left(v_i / V_i^2\right)}{2\mu}$$

$$R_{ij} = \frac{\left(mL_p|F|^2\right)_{ij}}{V_i^2}$$

$$I_{ij}^n = \frac{I_{ij}}{R_{ij}}$$

$$v_i = \frac{\overline{I_i^n}}{\sum_p \overline{I_p^n}}$$

I_{ij} = integrated intensity for Bragg peak j for phase I

R_{ij} = normalizing factor

I_{ij}^n = normalized intensity

K = instrument constant

m = multiplicity factor

L_p = Lorentz – polarization factor

$|F|$ = structure amplitude

V_i = unit cell of phase I

μ = linear attenuation coefficient

v_i = volume fraction of phase I

D.Y Li, B.H O'Connor, Q.T Chen, M.G Zadnik, *J Am. Ceram.Soc,* **77** [8] (1994)2195-98

JP Nicolich, Z Lences, W Dressler, R Riedel, *J. of Mat. Sci.* **35** (2000) 1427–1432

Effect of Reactive Pyrolysis Atmosphere

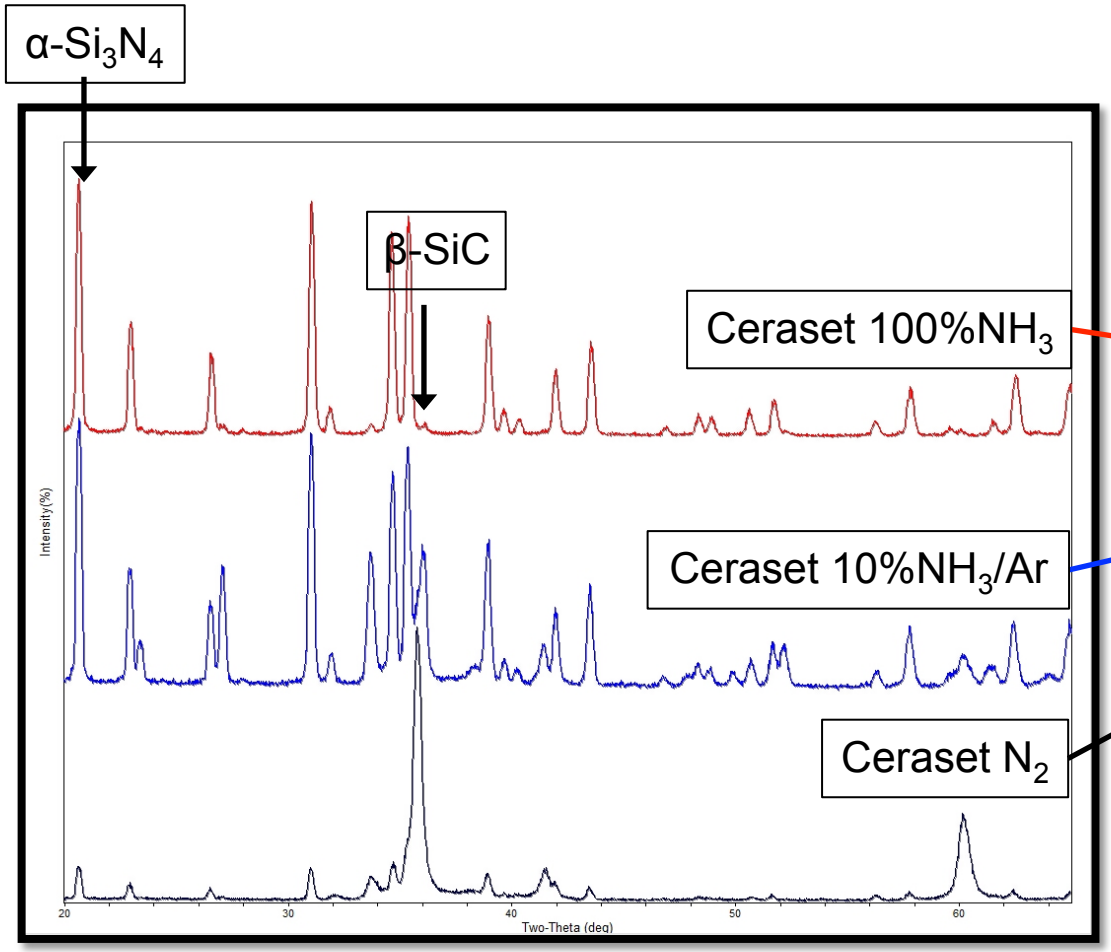

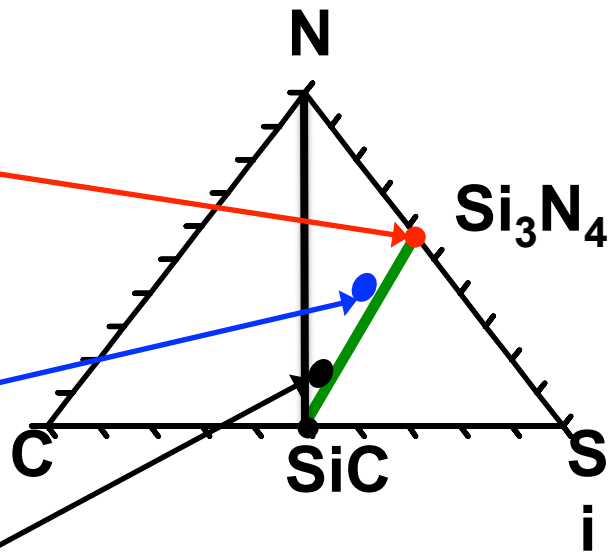

Following up on Riedel Group

Gas concentration during pyrolysis affects SiC content

Proposed Mechanisms

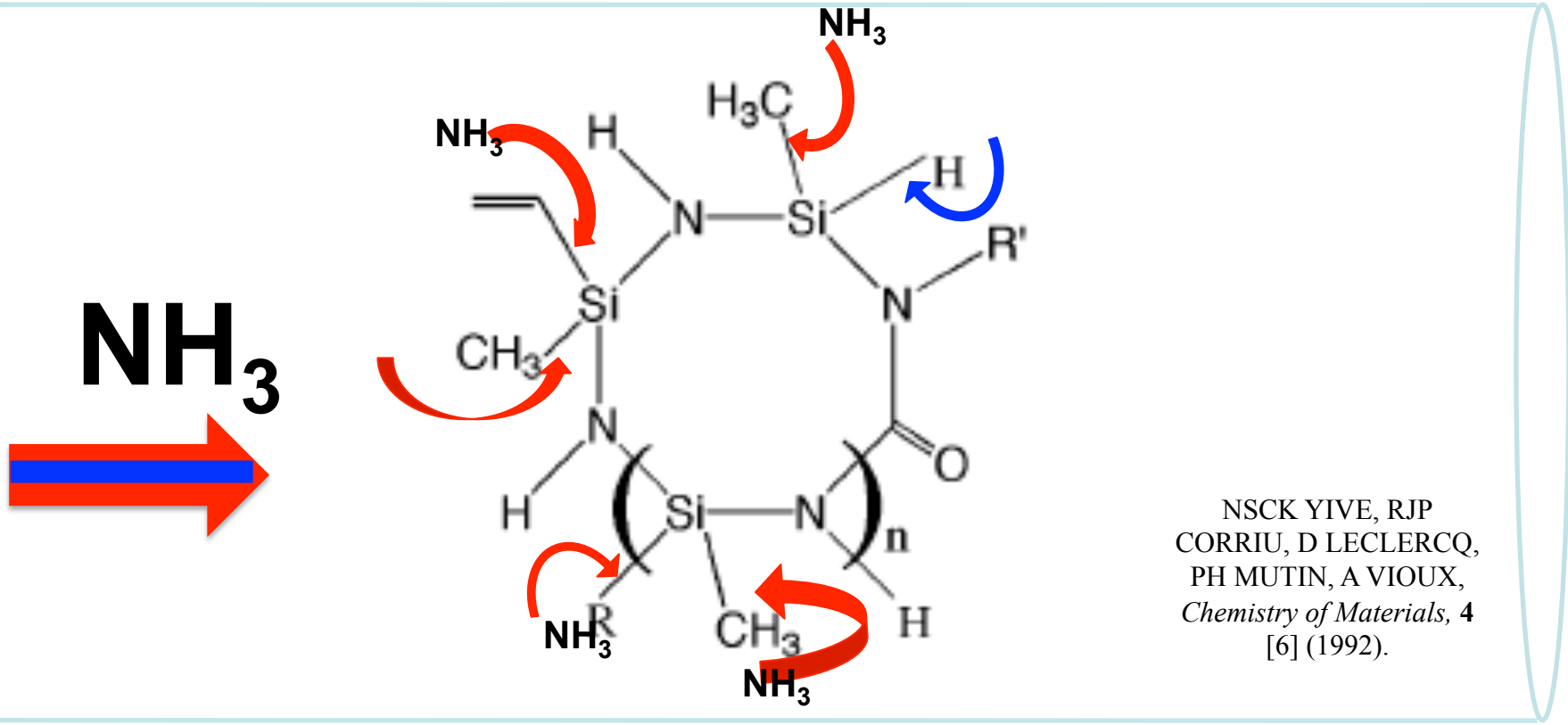

NSCK YIVE, RJP CORRIU, D LECLERCQ, PH MUTIN, A VIOUX, *Chemistry of Materials,* **4** [6] (1992).

NH_3 causes nucleophilic attack on Si-H bonds and homolytic cleavages on the Si-C bonds

Two-Step Pyrolysis

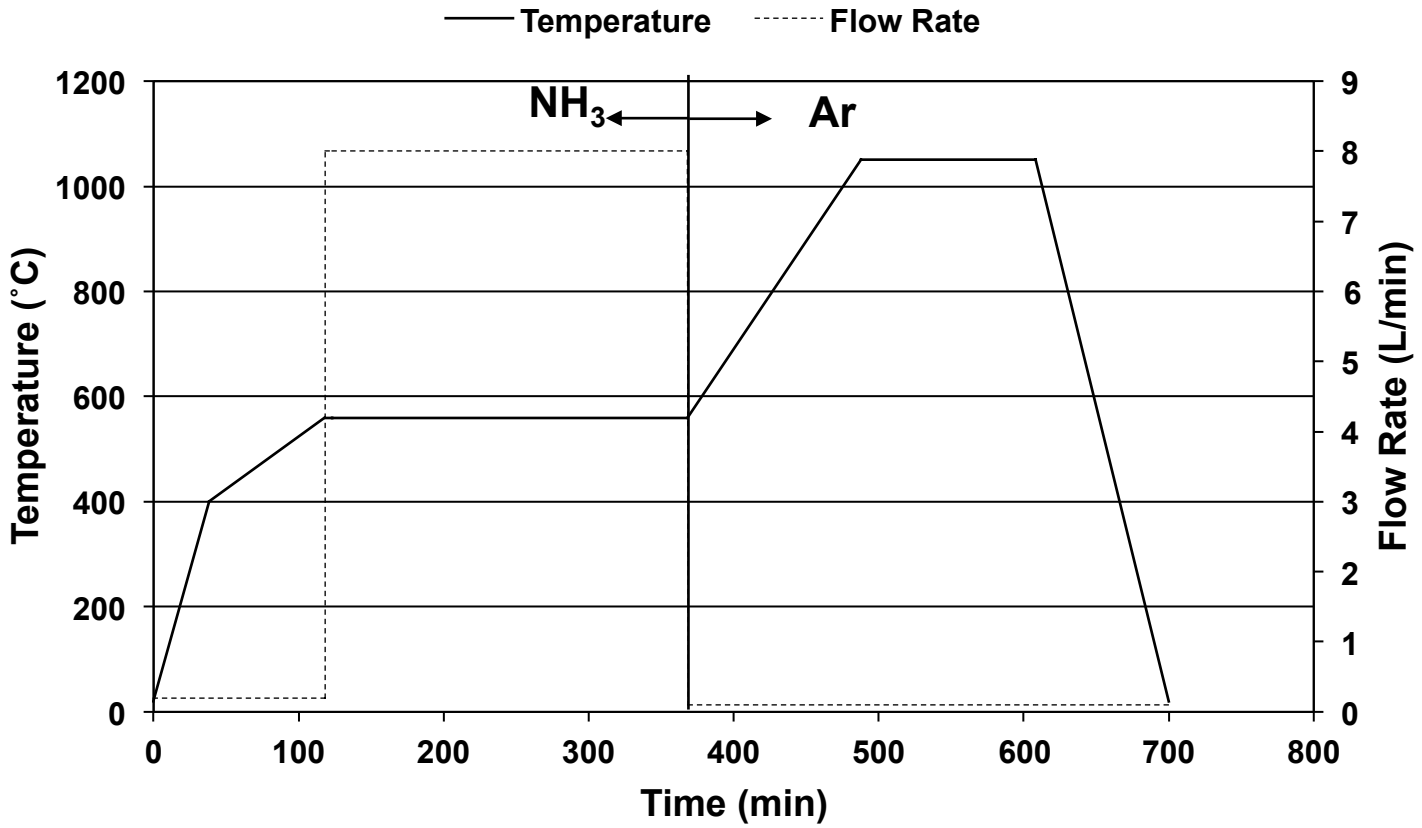

Flowing gas is switched from NH_3 to Ar at various temperatures and times to control the ratio of SiC/Si_3N_4

Time Effect of NH_3 Pyrolysis

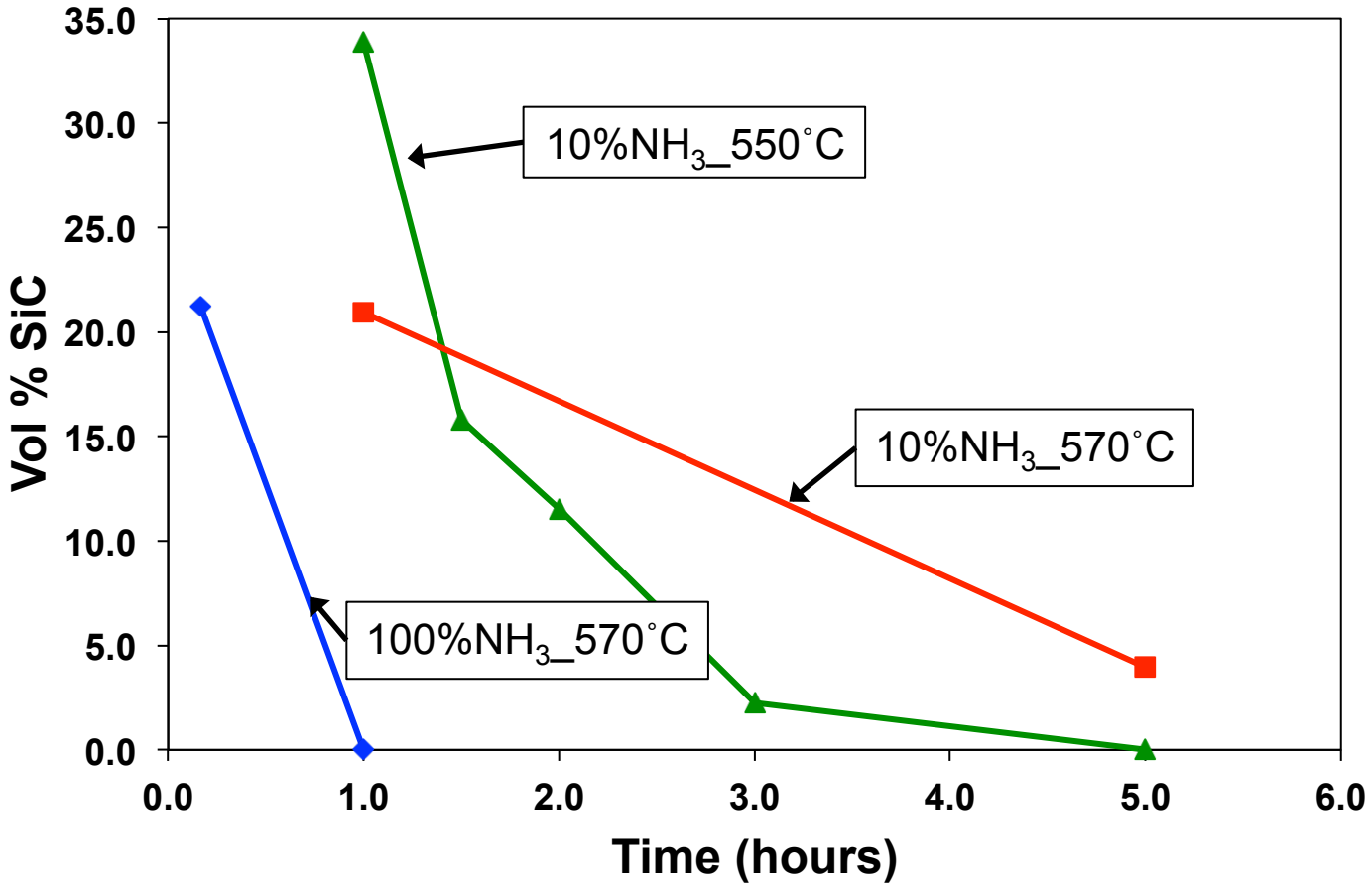

Controlled SiC content with varying time

Crystallite Size (after crystallization step (1650 ^{0}C in N_2))

Two-Step Pyrolysis	Phase	Volume %	Crystallite Size (nm)
10NH3_550C_1hr	beta - SiC	33.9	32
	beta - Si3N4	13.1	292
	alpha - Si3N4	53.0	550
10NH3_550C_1.5hr	beta - SiC	15.8	38
	beta - Si3N4	12.9	87
	alpha - Si3N4	71.3	687
10NH3_550C_2hr	beta - SiC	11.5	34
	beta - Si3N4	11.8	130
	alpha - Si3N4	76.7	750
10NH3_550C_3hr	beta - SiC	2.3	-
	beta - Si3N4	13.3	908
	alpha - Si3N4	84.4	1178
10NH3_550C_5hr	beta - SiC	0.0	
	beta - Si3N4	0.0	
	alpha - Si3N4	100.0	>1000

SiC is nano-scale and hinders the growth of Si_3N_4 grains

Status and Next Steps

Significant Accomplishment:

Developed the two-step pyrolysis process to control the SiC:Si_3N_4 in the desired range (0 – 25 % SiC)

Next Steps

- Gas Pressure Sintering Samples
  - 5, 10, 20, 30 v% SiC from the two-step pyrolysis process
  - 8 w% Lu_2O_3 sintering aid (based on results in the literature)
  - 1950 ˚C for 2 hours (based on preliminary results)
- FAST Sample
  - 5, 10, 20, 30 v% SiC from the two-step pyrolysis process
  - 8 w% Lu_2O_3 sintering aid (based on results in the literature)
  - 1700 ˚C for 10 min (based on preliminary results)
- Microstructural characterization and analysis
- Mechanical properties – room temperature modulus, strength and toughness; and high temperature creep

Composite Ceramic Coatings (summary)

I. Processing of composite ceramic coatings

- Cracking during constrained pyrolysis - critical coating thickness
- Control of coating thickness

II. Performance and applications of polymer derived ceramic coatings

- Oxidation protection of metals
- Joining of ceramics and fiber-reinforced ceramic matrix composites
- Control of surface energy

In the early stages (first eighteen months) of this project, due to the unavailability of silazane polymers, research was focused on siloxane derived composite ceramic coatings

Processing of Composite Ceramic Coatings

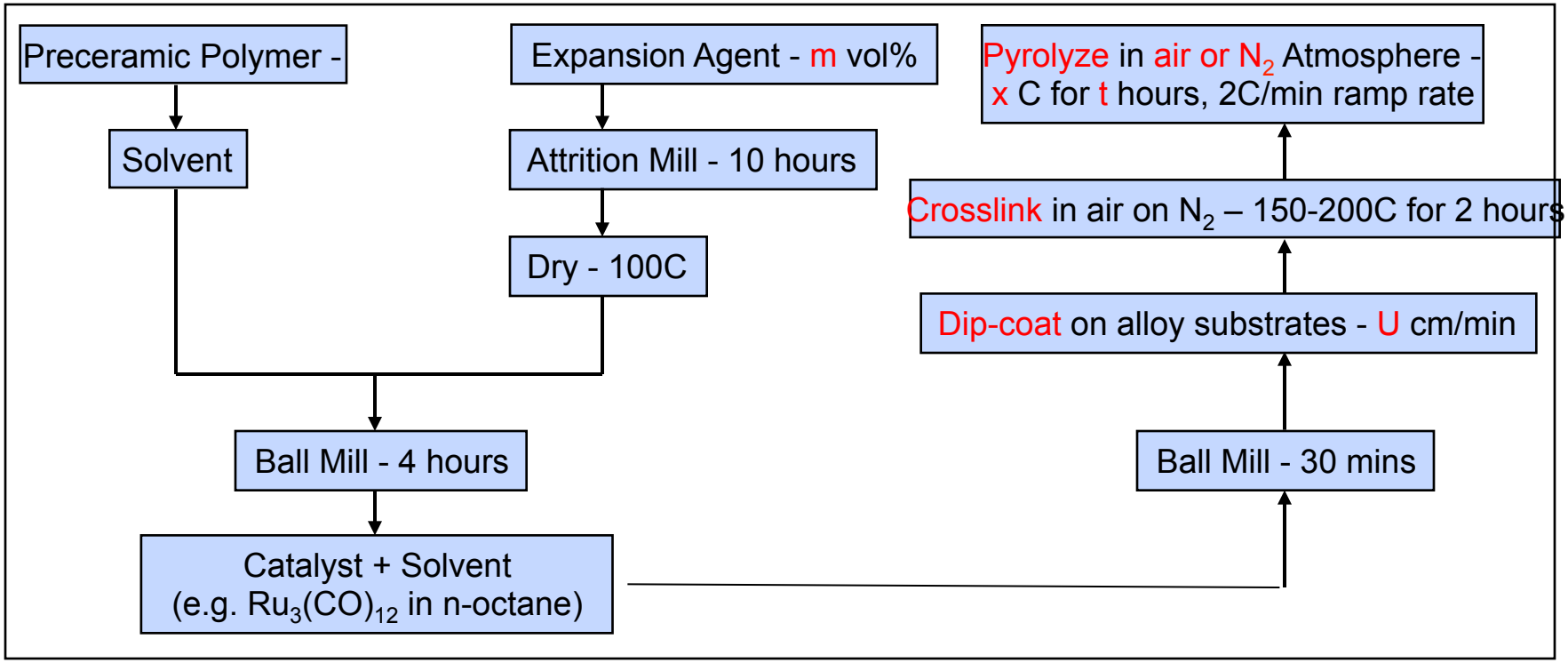

Volume fraction of the active filler in the range of 25 to 40 vol %

Cracking During Constrained Pyrolysis

Cracks observed in the some coatings after pyrolysis (classical mud-cracks)

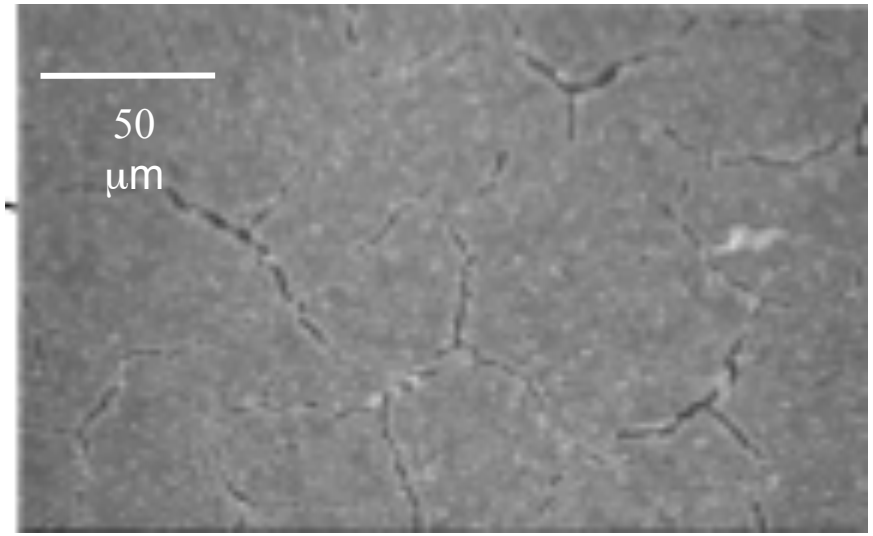

Conducted a mechanics based analysis to understand this

Calculated a critical coating thickness, T_{crit}, such that if $T < T_{crit}$, no cracking during constrained pyrolysis

The most important parameter that controls T_{crit} is the unconstrained shrinkage (and shrinkage rate) of the coatings

Critical Coating Thickness (Polysilazane with active fillers)

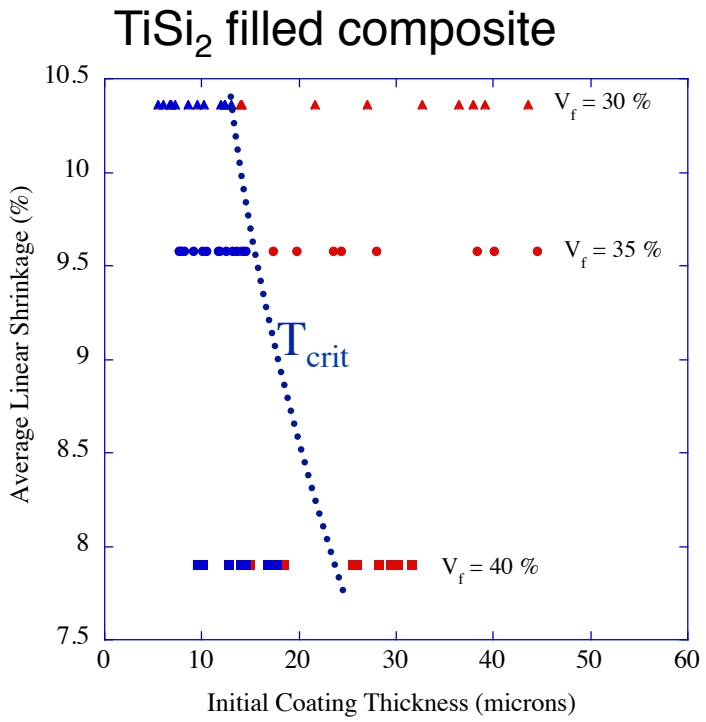

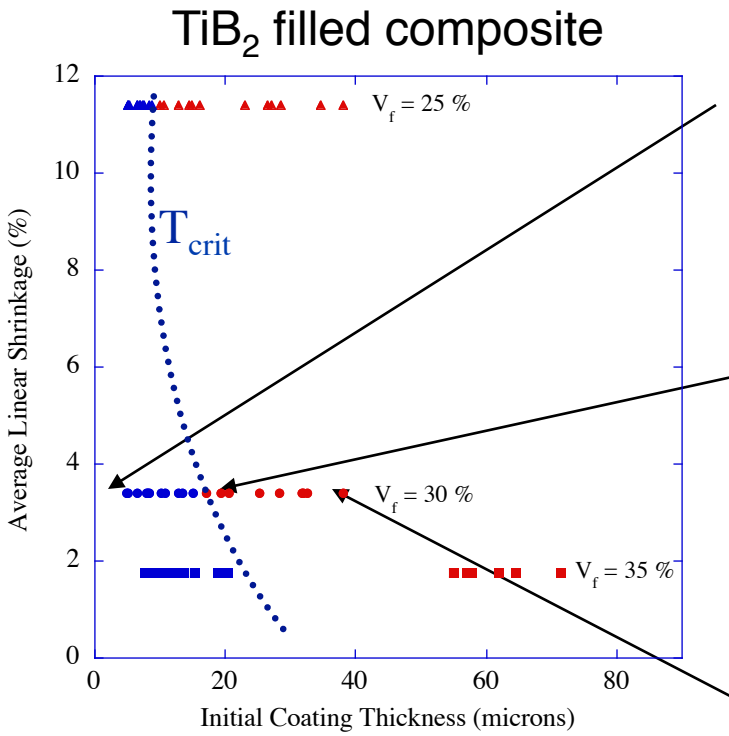

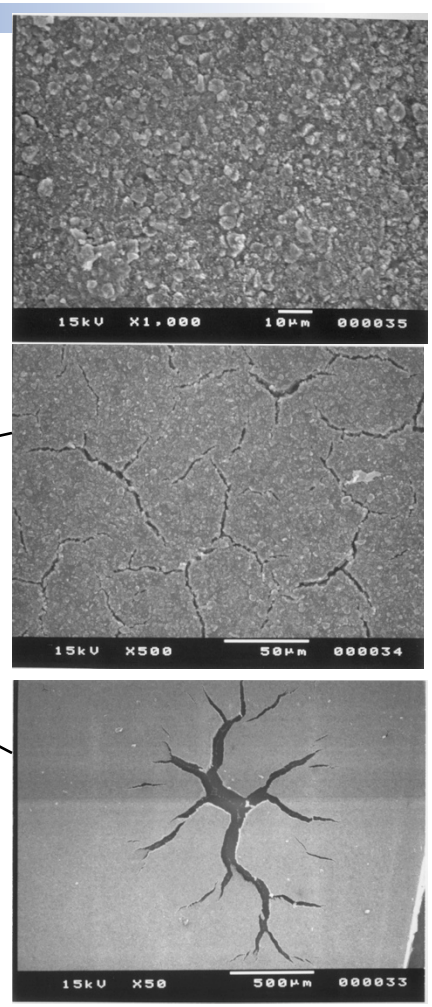

In the composite coatings if $T < T_c \rightarrow$ no cracking of coatings

Shrinkage rate controlled by filler volume fraction (V_f)

As volume fraction of filler ↑ , critical coating thickness ↑

- A critical coating thickness exists below which defect free coatings are obtained
- Initial filler volume fraction of fillers controls critical coating thickness

Thickness Control (Dip-Coating)

Modified Landau-Levich Analysis

- Pre-pyrolysis coating thickness as a function of dip coating withdrawal speed * at a slurry viscosity of 15cP and density of 1.34g/cm^3
- Linear shrinkage during pyrolysis
- To predict final coating thickness combine Eqns. 1 and 2 using following relationship:

$$t_0 = 0.2274\left(\frac{\mu_0 U}{g\rho}\right)^{\frac{n}{2}} + 4.918$$

$$\varepsilon_t = \frac{t_f - t_0}{t_0} = A\ln\left(t_0\right) - B$$

$$t_f = t_0\left(1 - \varepsilon_t\right)$$

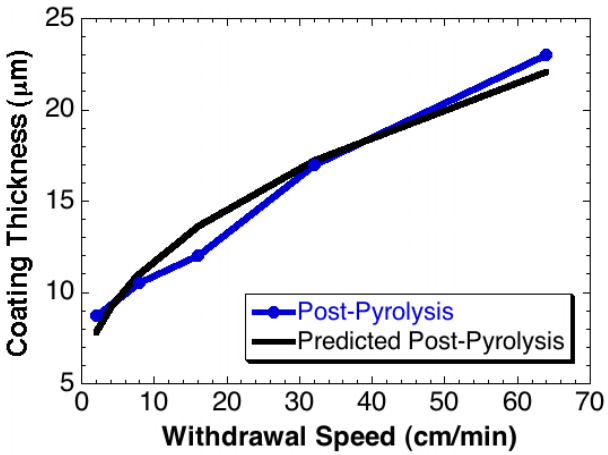

μ_0 = slurry viscosity (high rate)
U = withdrawal speed
g = gravity
ρ = density of slurry
n = shear thinning exponent of slurry

t_0 = initial thickness
t_f = final thickness
ε_t = linear strain
A,B = fitting parameters

$TiSi_2$-Filled PHMS Coatings on Steel

Submicron Filler- 30 vol%

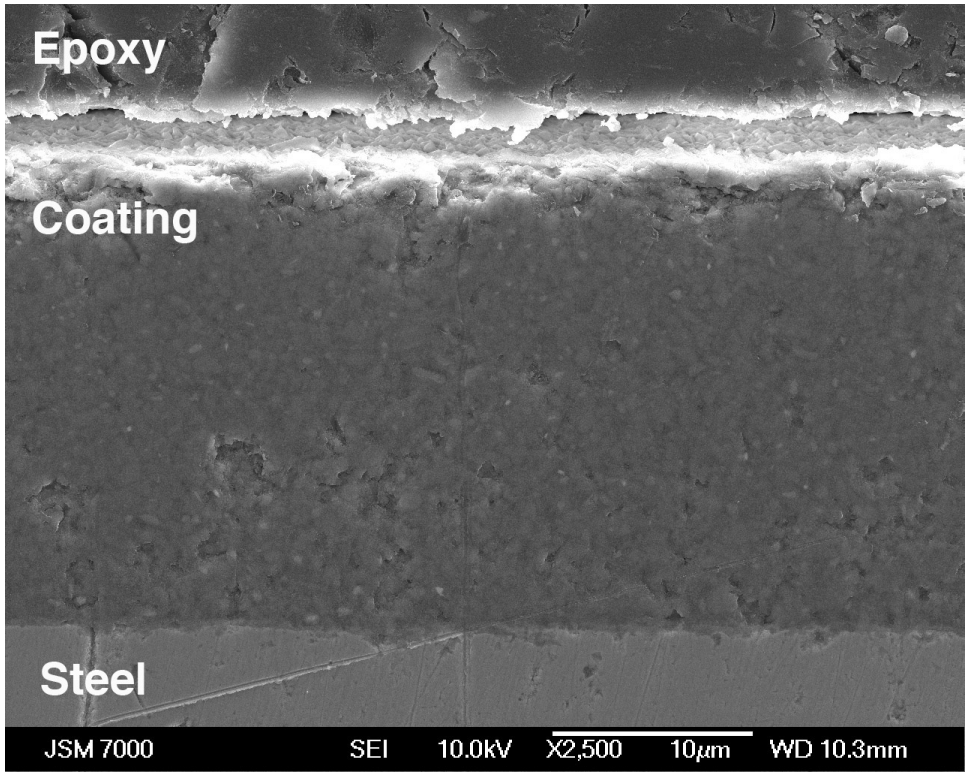

Approx. Composition by wt: 40% Si, 25% Ti, <5% C, balance O

Achieved a uniform thickness of 15-30 μm

Full conversion of submicron expansion agent

Coating still contains some porosity

Good bonding seen between coatings and substrate

Static Oxidation Protection of Inconel 617

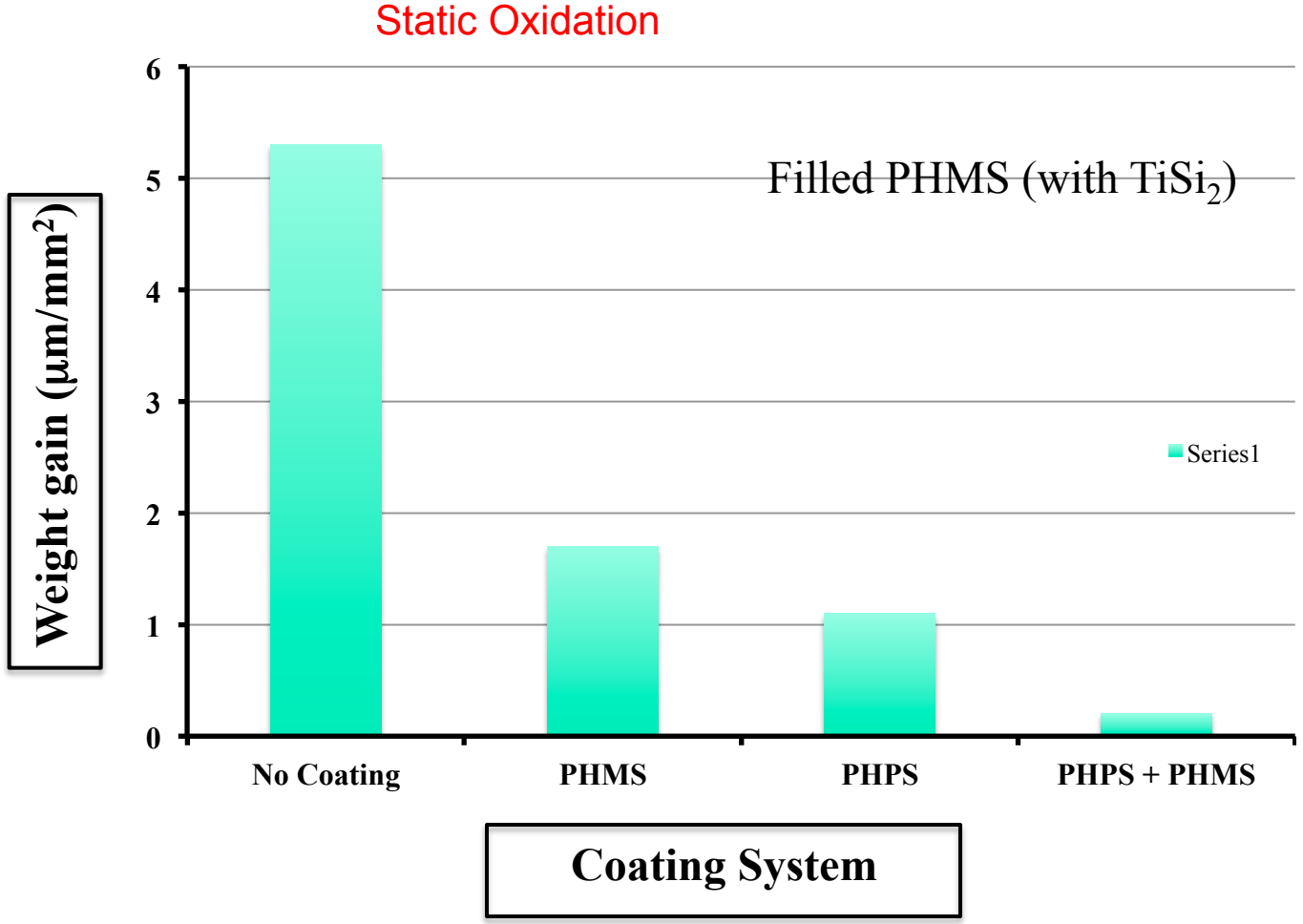

- 200 hours at 800ºC at 5ºC/min heating and cooling rates
- Coatings, especially the dual coating system provides excellent oxidation protection

Joining Ceramics and CMCs

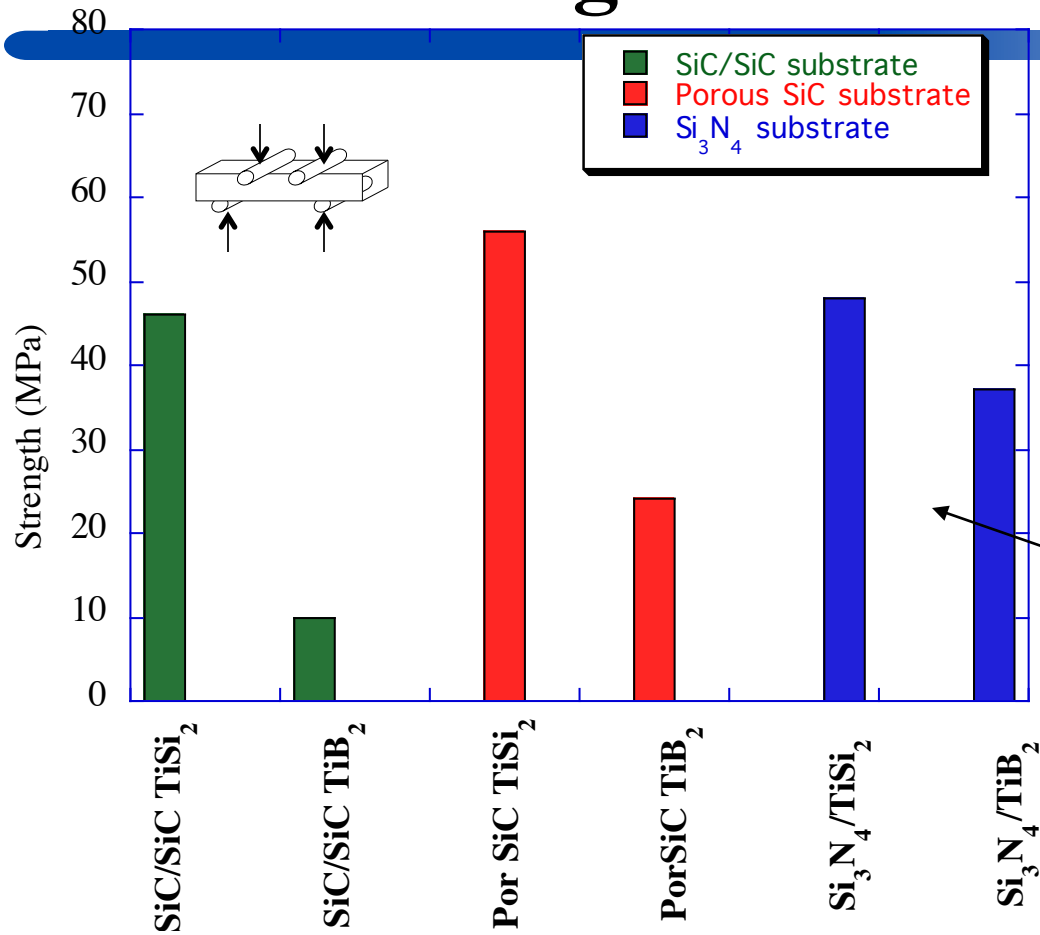

Typical joint cross section

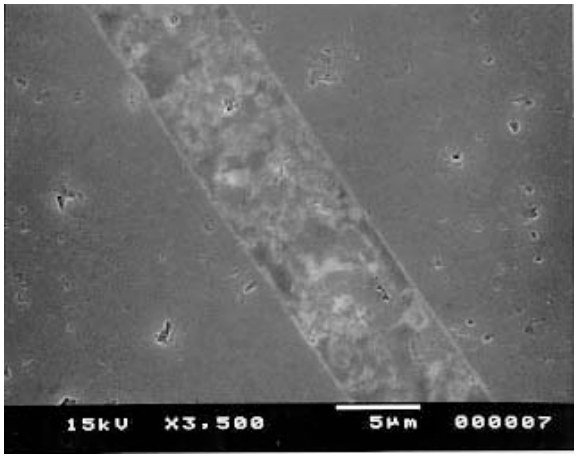

Typical joint failure surface

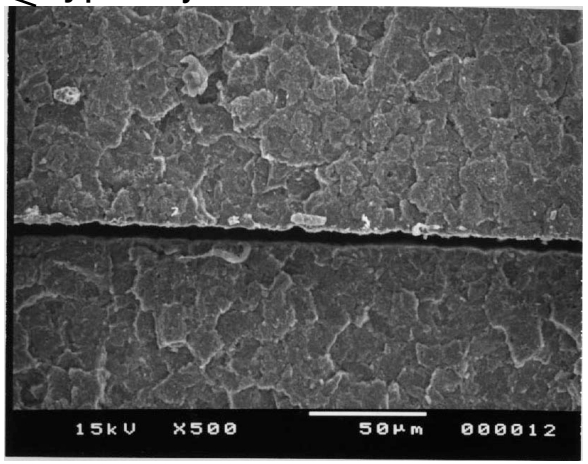

- Filled polysilazane joints
- Promising room temperature joint strengths
- Joining at low temperatures (1200 ^{0}C) and pressureless
- Joints failed in the joint material - not at the interface

Mixed Mode Fracture Toughness of Joints - Technique

Monolithic ceramic

crack grows in Mode I direction

At interface

- crack confined to interface if interfacial K_{IC} lower than bulk
- Interfacial toughness (G_i) depends on the loading phase angle (ω)

(where ω is $\tan^{-1} K_{II}/K_I$) $\omega = 0$: pure mode I loading

$\omega = 90$: pure mode II loading

G_i vs ω curve is necessary to characterize a given interface.

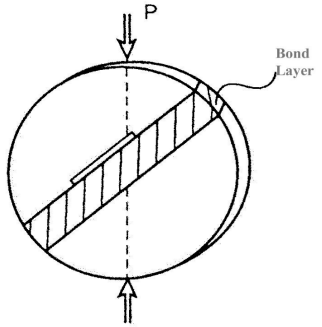

Brazil Nut Geometry

(test geometry chosen to obtain G_i as a function of phase angle)

- the loading phase angle is controlled by the compression angle.
- a large range of phase angles ranging from $-\pi/2$ to $\pi/2$ are possible
- ease of loading of the specimen (compared to other geometries)

Mixed Mode Fracture Toughness of Joints - Results

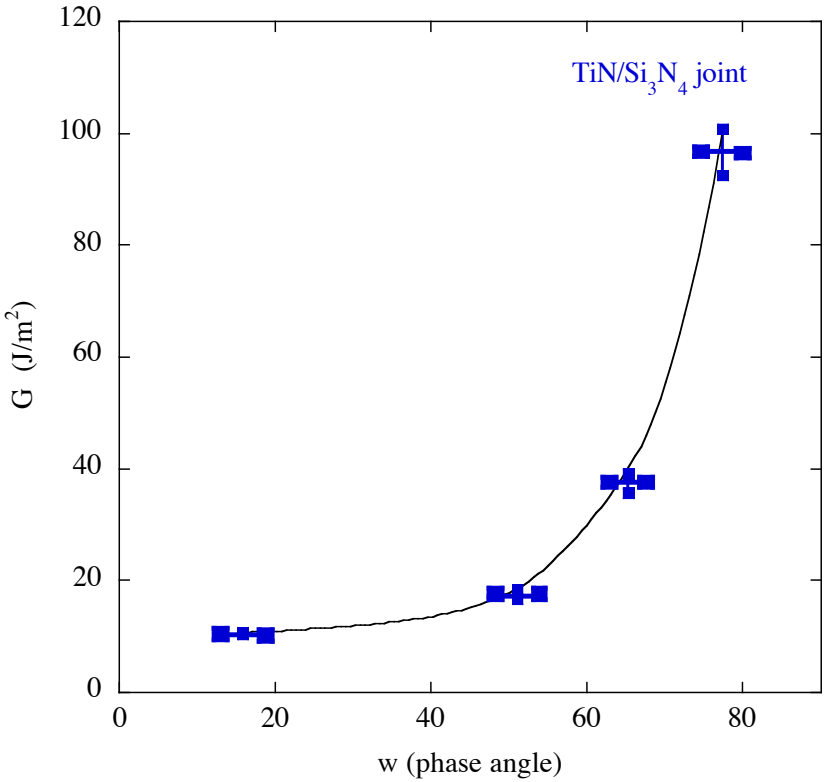

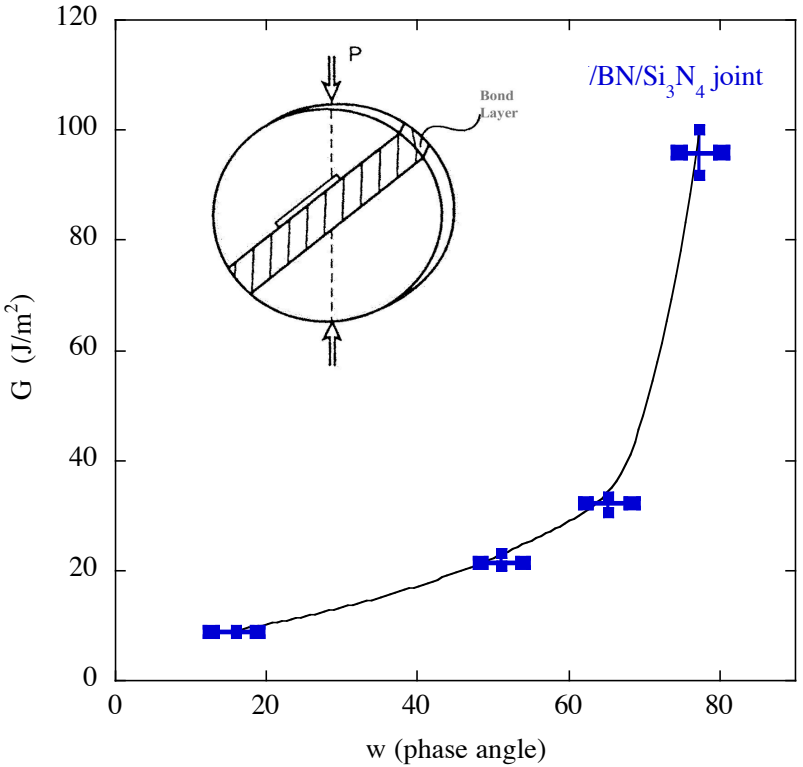

SiC joined with filled Ceraset

- Interfacial toughness increases with phase angle
- In all cases the samples failed at the interface

Mixed Mode Fracture Toughness of Joints - Analysis

Magnitude of crack shielding induced by asperities at the fracture surface is governed by the loading phase angle and a non-dimensional material parameter χ (Evans *et al*)

$$\chi = \frac{EH^2}{LG_o}$$

H is the roughness amplitude, L is the roughness wavelength
E is the elastic modulus.

when χ is small or ψ is zero
(H ⇨ 0 or L ⇨ ∞) no shielding

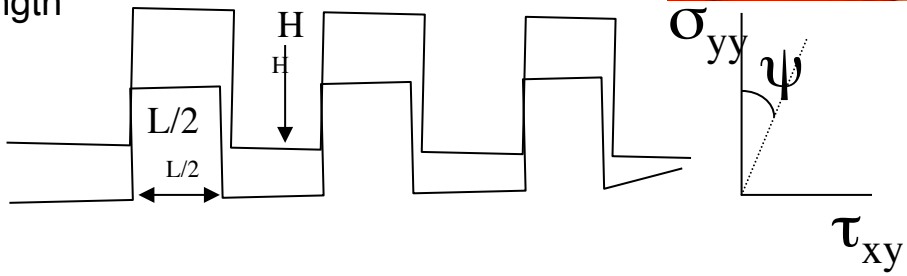

Measure H and L on the fracture surface using laser profilometery

Joint starting filler composition	H (average) (microns)	G_o J/m^2	E (GPa)	L (microns)	$\chi = EH/LG_0$ (experimental)
$TiSi_2$ filled joint	3.5	10	100	300	~ 400
TiB_2 filled joint	3.5	8.5	80	300	~ 380

- Shielding will strongly depend on the interface roughness (i.e. the magnitude of H and L).
- Model attempts to explain what is happening at the microstructural level during fracture.

Mixed Mode Fracture Toughness of Joints

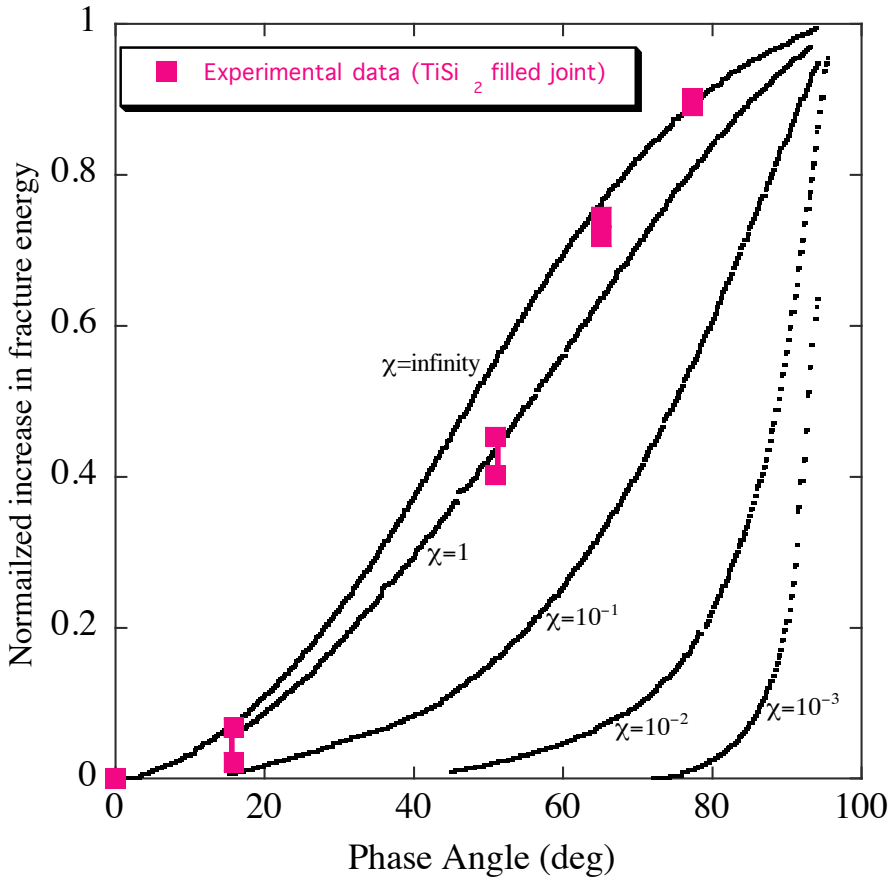

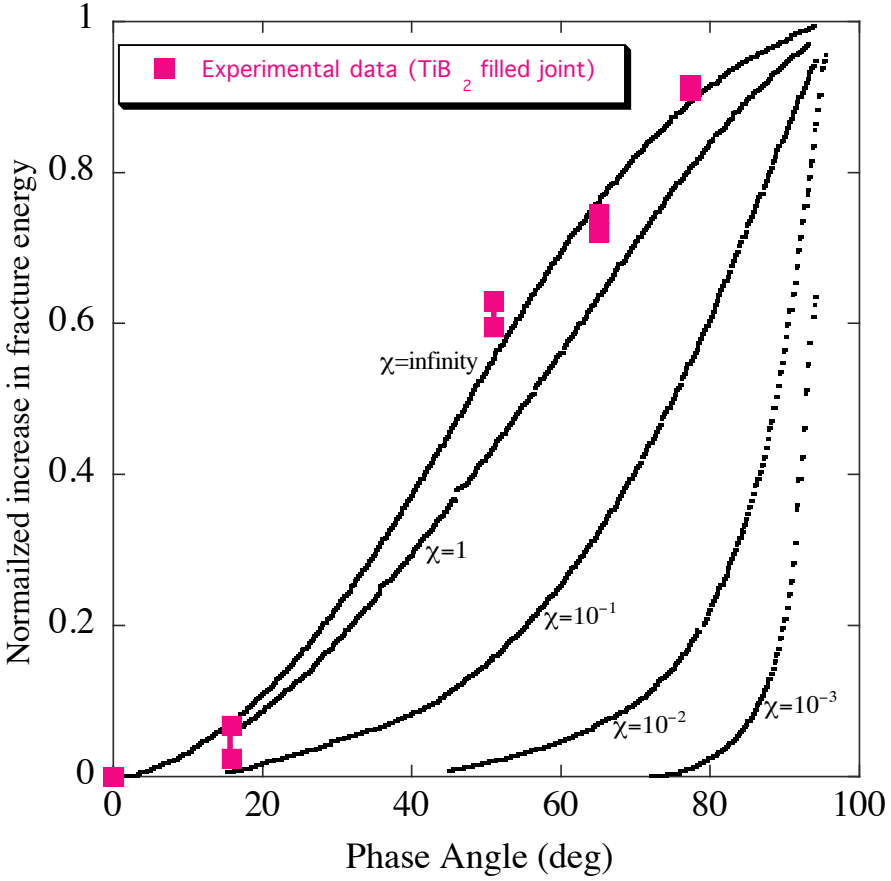

$$G^{*}(\omega) = \frac{G(\omega) - G(\omega = 0)}{G(\omega = 90) - G(\omega = 0)}$$

Normalized increase in fracture energy

- **Model is in agreement with values of χ obtained experimentally (~400)**
- **Model explains the role of asperities in controlling the interfacial fracture toughness.**

Control of Surface Energy (PHPS Films)

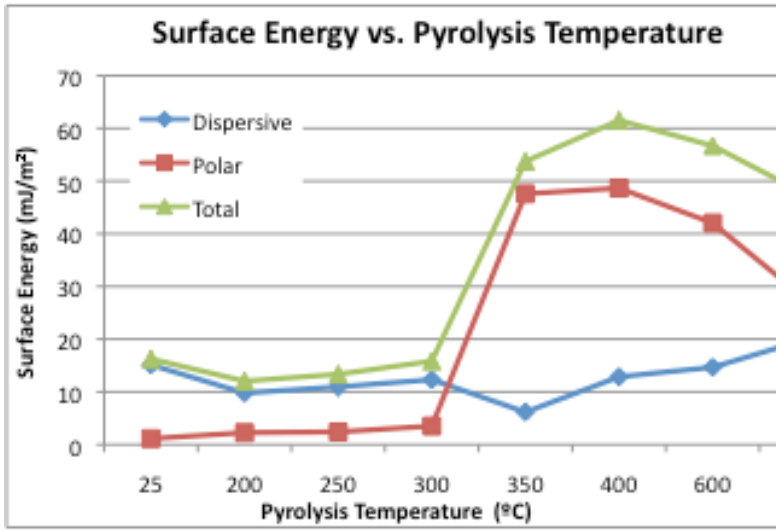

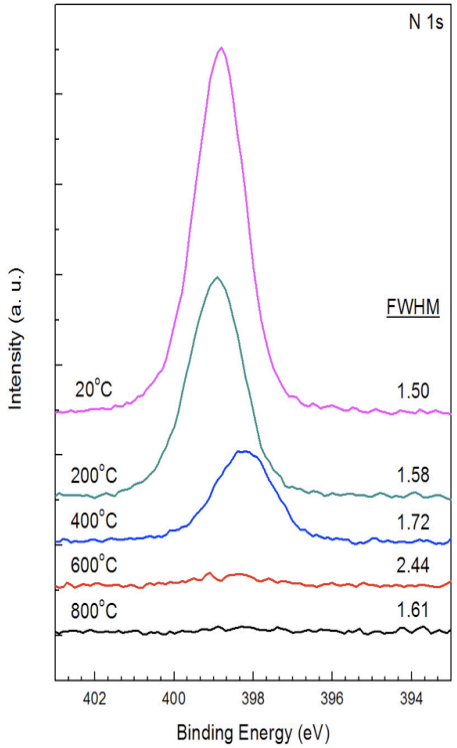

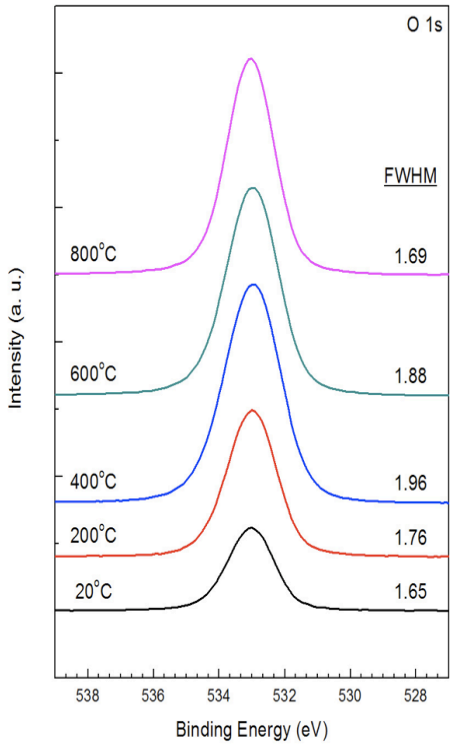

Significant change in surface energy around 300 ^{0}C: the major change is in the polar component
The change is due to replacement of Si-N bonds by Si-O bonda

Surface changes from hydrophobic (contact angle with water around 100 ^{0} to hydrophilic (contact angle around 40 ^{0})

Summary of Composite Coatings

- Analysis of constrained pyrolysis – critical coating thickness
- Development of an anlysis and experimental procedure to control coating thickness accurately
- Coating systems developed to provide excellent oxidation protection to ferritic alloys and nickel based superalloys
- PDCs suitable for joining ceramics and ceramic composites
- Mechanical properties of joints investigated – strength and fracture toughness
- A system developed in which surface energy can be controlled in a predictable manner

Summary of Accomplishments

- 8 papers in which this support has been acknowledged (more planned)
  - 4 published or accepted, 4 currently under preparation
- 3 papers by the Tomar group on materials produced by Bordia's group
- 16 invited talks in which this support has been acknowledged
- Partially supported 2 PhD students and 1 post-doc.

Acknowledgement

AIR FORCE OFFICE OF SCIENTIFIC RESEARCH
UNITED STATES AIR FORCE

Thanks for your attention